Robotica: (2020) volume 38, pp. 1105–1122. © Cambridge University Press 2019
doi:10.1017/S0263574719001279

Lyapunov-Based Formation Control of Underwater Robots

Ali Keymasi Khalaji* and Rasoul Zahedifar

Department of Mechanical Engineering, Faculty of Engineering, Kharazmi University, Tehran, Iran

(Accepted July 18, 2019. First published online: August 15, 2019)

SUMMARY
Today, automatic diving robots are used for research, inspection, and maintenance, extensively. Control of autonomous underwater robots (AUVs) is challenging due to their nonlinear dynamics, uncertain models, and the system underactuation. Data collection using underwater robots is increasing within the oceanographic research community. Also, the ability to navigate and cooperate in a group of robots has many advantages compared with individual navigations. Among them, the effectiveness of using resources, the possibility of robots' collaboration, increasing reliability, and robustness to defects can be pointed out. In this paper, the formation control of underwater robots has been studied. First, the kinematic model of the AUV is presented. Next, a novel Lyapunov-based tracking control algorithm is investigated for the leader robot. Subsequently, a control law is designed using Lyapunov theory and feedback linearization techniques to navigate a group of follower robots in a desired formation associated with the leader and follow it simultaneously. In the obtained results for different reference paths and various formations, the effectiveness of the proposed algorithm is represented.

KEYWORDS: Underwater robot; Formation control; Multiagent AUVs; Trajectory tracking.

1. Introduction

Robotics as an important field of research is growing in interest within the research community.[1–5] In recent years, autonomous underwater robots (AUVs) have played an important role in underwater researches and explorations. These robots replaced human resources in many activities such as undersea and ocean commercial and scientific researches and mapping. Scientists employ AUVs to study lakes', seas', and oceans' floor. As an example, AUVs have been used to find wreckages of missing airplanes and ships in oceans and seas. The oil and gas engineering also utilizes AUVs to make detailed plans of the seafloor before they start constructing subsea infrastructures. The ability of high-tech AUVs as well as their superiority to humans in oceanic missions, especially at high depths, has made these robots a key player in the underwater industry.[6] The main focus of the study on AUVs is the existence of various constraints in the modeling of these systems. Nonlinear equations, uncertainties, and the dependence of model parameters on environmental configurations, as well as the presence of external disturbances caused by ocean flow dynamics, make controlling of these systems very attractive and complicated at the same time. Therefore, dynamic analysis and designing control algorithms for these systems have attracted the attention of researchers. There are many research efforts in the fields of modeling, control methods, and system identification to enhance the autonomy of these devices. Different control methods have been suggested such as sliding mode control,[7,8] higher-order sliding mode control,[9] terminal sliding control,[10] adaptive control,[11–16] neural network control, and[13–15,17] fuzzy control.[18] In this paper, a novel Lyapunov-based tracking control algorithm is designed for the AUV using the separation of the system kinematics and dynamics.

* Corresponding author. E-mail: keymasi@khu.ac.ir

One of the key issues in the context of robotics is the control of a group of robots in tracking reference trajectories. A multiagent system is made up of a set of mobile robots, that is, several agents that exist at the same time, share common resources, and communicate with each other. The key issue in multiagent systems is the coordination between agents. A multiagent system is a group of several intelligent agents, each acting toward its objectives, while all cooperating in a common environment, being able to communicate, and possibly organizing their actions. This capability to plan ahead is considered as a complex cognitive skill, and it appears from the communications between the individuals in the group. The robots are able to plan a sequence of activities, which no individual in the group would be able to do alone. Meanwhile, in some complex and specific environments, multiple robots have more advantages than a single one. Ability to navigate and cooperate in a group of robots has many advantages compared with individual navigation including the efficiency of using resources (such as sharing the use of sensors), robot parallelism, safety, and fault tolerance increase. Meanwhile, in some complex and specific environments, multiple robots have more advantages than a single one. In addition, more aircraft collaboration means more different equipment that can be carried on to accomplish more difficult tasks. Therefore, the design of the multiagent intelligent systems has attracted many scholars.

The idea of controlling the formation of robots can be found in the biology sciences. Researchers in the biological sciences have seen some types of formed behaviors in nature. They found that animals form groups so that they can more effectively exchange their findings in those groups. In this way, they can find more foods and protect themselves against possible dangers.[19] One of the noteworthy points in the lives of these animals is the preservation of personal territory and life at a certain distance from the neighbors simultaneously with the presence of the group.[20,21] More examples in terms of using formation of robots compared to individuals can also be expressed in search and rescue missions,[22–24] automated guidance systems on highways,[25] and air traffic control.[26] Some of the other applications include utilization in inaccessible and hostile environments such as space or purification of toxic and hazardous chemicals, exploration and destruction of mines and caves, and identification and investigation in battlefields.[27] Various methods have been utilized for the formation control of smart robots. In general, these methods seek to create a good arrangement by coordinating mobile robots. The methods used to control formation can be divided into three general categories including virtual structure approach,[28,29] behavior-based approach,[30–32] and leader–follower approach.[33,34]

Among these methods, leader–follower approach has attracted many researchers.[35,36] In the leader–follower approach, some agents are considered as leaders, while others act as followers which track the leaders with a predefined offset. In this approach, a leader follows its desired trajectory, while follower robots track the position of the leader. In this method, the robot configuration is fully determined by the position of the leader robot. The leader–follower approach is mostly appreciated because of its simplicity and scalability.[37] The important benefits of this method are simplicity, high reliability, and low computational cost.[38] Another advantage is that only the leader is responsible for planning trajectories and followers must follow the coordinates of the leader with a predefined offset; therefore, it leads to a simple approach. The independence of followers is another benefit of this method. In the leader–follower approach, angle–distance or distance–distance models can be used. In the angle–distance model, robots are controlled as a chain loop, in which each robot follows a leader. In the distance–distance model, each robot simultaneously tracks two robots. The formation control of a group of robots can be achieved in a variety of linear and columnar modes and so on. In ref. [39], a control model was developed using graphs theory for a group of robots that could provide an appropriate formation for passing obstacles. In ref. [40], a fuzzy sliding mode algorithm is also proposed.

In the behavior-based approach, several reactive behaviors are prescribed (e.g., move-to-goal, avoid-robot, avoid-static-obstacles, and maintain-formation). The action of each agent is derived by a weighted sum of all the behaviors. Robot's final action is derived by weighting the relative importance of each behavior. The theoretical formalization and mathematical analysis of this approach are difficult and consequently it is not easy to guarantee the convergence of the formation to a desired configuration. The restriction of behavior-based approach is that it is challenging to be evaluated mathematically; therefore, it is hard to assure a precise formation control. The main problem with this method is that it is difficult to formulize the formation mathematically, and the team of agents is not guaranteed to converge to the desired formation. This technique has some drawbacks such as the need to developing a mathematical model of the group dynamics, studying the convergence of specific formation, and ensuring the stability of the entire formation.

https://doi.org/10.1017/S0263574719001279 Published online by Cambridge University Press

The virtual linkage approach considers the entire formation as a single rigid body and is able to maintain the formation shape in high precision during maneuvers. In this case, the behavior of the robot formation is predictable and consequently the control of the robot formation is straightforward. Nevertheless, a large inter-robot communication bandwidth is required. The main drawback of the virtual structure implementation is the centralization, which leads to a single point of failure for the entire system. Another criticism of the virtual structure approach is that it has poor reconfiguration capacity and needs to refresh the relative positions of all the team members when the formation pattern changes. Furthermore, heavy communication and computation burden is concentrated on the centralized location, which may reduce the whole system's performance.

In the leader–follower approach which is focused in this paper, one of the robots in the group is considered as the leader and others are required to follow the leader. As a result, the problem of formation control of the multiagent robotic systems turns into two simpler problems. One is the tracking control of the leader, and the other is maintaining the formation by the other agents. Follower robots are required to form and maintain the desired formation and to adjust their position according to the position of the leader. Thus, in order to regulate a formation maneuver, it is only necessary to specify the relative position between the leader and the follower robot. In this paper, a Lyapunov-based leader–follower approach is designed for the formation control of a group of AUVs.

First, the kinematic model of an AUV is extracted, and reference paths are developed to track by the leader robot. Then, a kinematic control law was developed for the leader robot to asymptotically follow the reference trajectories, and the stability is investigated through the Lyapunov method. In the following, a dynamic controller is designed for the leader robot to produce required operating torques. Subsequently, the problem of controlling the formation of the leader and follower AUVs is analyzed. The required control algorithm for the follower AUVs has been obtained to maintain their formations associated with the leader robot. The results show the effectiveness of the designed control algorithm. The main contributions of this paper are as follows:

- investigating a novel Lyapunov-based tracking control algorithm for the AUV, using the separation of the kinematics and dynamics;
- designing a formation control law for tracking control of the AUV;
- analyzing the stability of the closed loop control system;
- presenting several case studies for the system performance in order to show the effectiveness of the proposed method.

2. AUV Kinematic Model

AUVs are a subset of mobile robotic systems. A schematic diagram of an AUV is shown in Fig. 1. Two coordinate systems are used to introduce the system. The moving coordinate system, which is usually considered in the robot's center of gravity, describes the system motions with respect to a fixed coordinate system.

In this paper, the robot's motion is only evaluated on the horizontal plane and its roll and pitch motions are neglected. Therefore, for the evaluation of the dynamic and kinematic equations, only three independent components are needed as $q = \begin{bmatrix} x\ y\ \varphi \end{bmatrix}^T$, where $\begin{bmatrix} x\ y \end{bmatrix}^T$ is the coordinate of point P in the fixed frame and φ is the angle between the longitudinal axis of the robot and X axis. The relationship between the linear and angular velocities of the AUV in the fixed coordinate system is expressed by the kinematic model as

$$\begin{cases} \dot{x} = u\cos\ \varphi\ - v\sin\ \varphi \\ \dot{y} = u\sin\ \varphi\ + v\cos\ \varphi \\ \dot{\varphi} = r \end{cases} \tag{1}$$

where u, v, and r are the generalized velocities in $\boldsymbol{X}$, $\boldsymbol{Y}$, and $\boldsymbol{Z}$ directions, respectively.

3. AUV Dynamic Model

In order to calculate system dynamic equations, the AUV is assumed as a rigid body and the dynamical equations are obtained based on the Newton–Euler method. In the calculation of system mathematical model, the hydrodynamic effects and the external forces and torques exerted on

https://doi.org/10.1017/S0263574719001279 Published online by Cambridge University Press

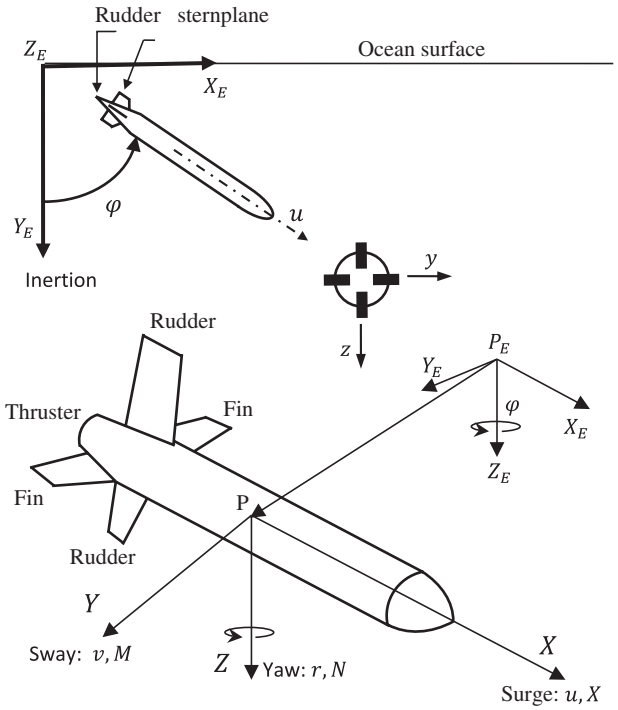

Fig. 1. The AUV in motion plane.

the AUV are taken into account. Therefore, the dynamical equations of the system can be obtained as:[41]

$$\begin{bmatrix} \dot{u} \\ \dot{v} \\ \dot{r} \end{bmatrix} = A \begin{bmatrix} u \\ v \\ r \end{bmatrix} + B \begin{bmatrix} vr \\ ur \\ uv \end{bmatrix} + D \begin{bmatrix} u\,|u| \\ v\,|v| \\ r\,|r| \end{bmatrix} + H \begin{bmatrix} F_u \\ F_v \\ \tau_r \end{bmatrix} \tag{2}$$

where u, v, and r are the generalized velocities, which are shown in Fig. 1, and $\dot{u}$, $\dot{v}$, and $\dot{r}$ are their time derivatives, respectively. Also, $A = \text{diag}\left[\frac{X_u}{X_{\dot{u}}-m} \; \frac{Y_v}{Y_{\dot{v}}-m} \; \frac{N_r}{N_{\dot{r}}-I_z}\right]$; $B = \text{diag}\left[\frac{m-Y_{\dot{v}}}{m-X_{\dot{u}}} \; \frac{X_{\dot{u}}-m}{m-Y_{\dot{v}}} \; \frac{Y_{\dot{v}}-X_{\dot{u}}}{I_z-N_{\dot{r}}}\right]$; $D = \text{diag}\left[\frac{X_{u|u|}}{X_{\dot{u}}-m} \; \frac{Y_{v|v|}}{Y_{\dot{v}}-m} \; \frac{N_{r|r|}}{N_{\dot{r}}-I_z}\right]$; $H = \text{diag}\left[\frac{1}{m-X_{\dot{u}}} \; \frac{1}{m-Y_{\dot{v}}} \; \frac{1}{I_z-N_{\dot{r}}}\right]$
and diag(.) represents the diagonal matrix with the determined diameter elements.

4. Trajectory Tracking Control

The trajectory following is one of the control problems in autonomous navigation of AUVs. In this problem, it is desirable that the moving robot, starting from a certain initial condition, reaches the desired path in the Cartesian space and follows it with a definite timing. Therefore, control inputs try to make the system states asymptotically follow a series of desired states, and the tracking error $\left[x - x_d \; y - y_d\right]^T$ approaches to the origin gradually. The purpose of this section is to design the kinematic control input vector $\mathcal{V} = \left[u \; v \; r\right]^T$ in order to approach point P to the reference point $P_d = \left[x_d \; y_d\right]^T$.

4.1. Trajectory planning

It is assumed that the reference path in the Cartesian space to be followed by the robot is expressed as $x_d = x_d\,(t)$, $y_d = y_d\,(t)$, where d is used to represent the variables on the desired trajectory. The aim of this section is to map this path to the space of the robot variables. In this case, the generated paths for the robot will be traversable.
Using the kinematics equations of the system (Eq. (1)), reference trajectories $\varphi_d\,(t)$, $u_d\,(t)$, $v_d(t)$, and $r_d\,(t)$ can be easily obtained.

https://doi.org/10.1017/S0263574719001279 Published online by Cambridge University Press

Property 1. The reference signals $x_d(t)$, $y_d(t)$, and $\varphi_d(t)$ and the system reference kinematic inputs $u_d(t)$, $v_d(t)$, and $r_d(t)$ and their derivatives are continuous and globally bounded.

4.2. Kinematic control

In this section, a nonlinear Lyapunov-based tracking control is investigated for the AUV. Therefore, first the system error dynamics is described. The goal is to investigate a kinematic feedback control algorithm $\mathcal{V} = \mathcal{V}(q, q_d, \mathcal{V}_d)$ (where $\mathcal{V}_d = \begin{bmatrix} u_d & v_d & r_d \end{bmatrix}^T$ is the AUV velocity vector on the reference trajectory) for the AUV in order to stabilize the error vector defined as $\tilde{\mathbf{e}} = q - q_d$ at the origin. It is assumed that the robot state variables are measured at any instant of time with sensors and closed loop control inputs $\mathcal{V} = \begin{bmatrix} u & v & r \end{bmatrix}^T$ are generated using these signals. Therefore, the error signal can also be considered as

$$e = T(\varphi_d)\,\tilde{\mathbf{e}} \tag{3}$$

where the transformation matrix $T(\varphi_d)$ is chosen as

$$T(\varphi_d) = \begin{bmatrix} \cos\varphi_d & \sin\varphi_d & 0 \\ -\sin\varphi_d & \cos\varphi_d & 0 \\ 0 & 0 & 1 \end{bmatrix} \tag{4}$$

Therefore, Eq. (3) can also be expressed as

$$\begin{bmatrix} e_1 \\ e_2 \\ e_3 \end{bmatrix} = T(\varphi_d) \begin{bmatrix} x - x_d \\ y - y_d \\ \varphi - \varphi_d \end{bmatrix} \tag{5}$$

Differentiating in order to obtain system error dynamics yields

$$\begin{bmatrix} \dot{e}_1 \\ \dot{e}_2 \\ \dot{e}_3 \end{bmatrix} = \begin{bmatrix} -\dot{\varphi}_d \sin\varphi_d & \dot{\varphi}_d \cos\varphi_d & 0 \\ -\dot{\varphi}_d \cos\varphi_d & -\dot{\varphi}_d \sin\varphi_d & 0 \\ 0 & 0 & 0 \end{bmatrix} \begin{bmatrix} x - x_d \\ y - y_d \\ \varphi - \varphi_d \end{bmatrix} + \begin{bmatrix} \cos\varphi_d & \sin\varphi_d & 0 \\ -\sin\varphi_d & \cos\varphi_d & 0 \\ 0 & 0 & 1 \end{bmatrix} \begin{bmatrix} \dot{x} - \dot{x}_d \\ \dot{y} - \dot{y}_d \\ \dot{\varphi} - \dot{\varphi}_d \end{bmatrix} \tag{6}$$

Simplifications lead to the following error dynamics:

$$\begin{cases} \dot{e}_1 = r_d\, e_2 + u\cos e_3 \; - v\sin e_3 \; - u_d \\ \dot{e}_2 = -r_d\, e_1 + u\sin e_3 \; + v\cos e_3 \\ \dot{e}_3 = r - r_d \end{cases} \tag{7}$$

The obtained nonlinear error equations can be expressed as $\dot{e} = f(e, q_d, \mathcal{V}_d, \mathcal{V})$. The purpose is to obtain the closed loop control algorithm $\mathcal{V} = \mathcal{V}(q, \dot{q}, q_d, \mathcal{V}_d)$ in order to stabilize the system error dynamics. It is assumed that state transformations $z_1 = e_1$, $z_2 = e_2$, $z_3 = \tan e_3$ and input transformations $\Omega_1 = u\cos e_3 \; - u_d$, $\Omega_2 = v\cos e_3$, $\Omega_3 = \frac{\mathrm{d}z_3}{\mathrm{dt}}$ are applied to the system. It is worth noting that these transformations do not change system equilibrium point and can be considered as a diffeomorphism. Using these transformations yields

$$\begin{cases} \dot{z}_1 = r_d z_2 + \Omega_1 - \Omega_2 z_3 \\ \dot{z}_2 = -r_d z_1 + (u_d + \Omega_1) z_3 + \Omega_2 \\ \dot{z}_3 = \Omega_3 \end{cases} \tag{8}$$

The purpose is to design control inputs Ω_1, Ω_2, and Ω_3, in order to ensure the stabilization of $z_i (i\colon 1 \to 3)$. Therefore, the following inputs are proposed for the stabilization of the system (Eq. 8).

$$\begin{cases} \Omega_1 = -|u_d|\,(k_1 z_1 + k_2 z_2 z_3) \\ \Omega_2 = -|u_d|\,(k_2 z_2 + k_1 z_1 z_3) \\ \Omega_3 = -\frac{k_2}{k_3} z_2 u_d - |u_d| z_3 \end{cases} \tag{9}$$

where $k_i (i\colon 1 \to 3)$ are system positive control gains.

https://doi.org/10.1017/S0263574719001279 Published online by Cambridge University Press

Using inverse transformations, system kinematic control inputs can be obtained as

$$\begin{cases} u = \frac{\Omega_1 + u_d}{\cos e_3} \\ v = \frac{\Omega_2}{\cos e_3} \\ r = \Omega_3 + r_d \end{cases} \tag{10}$$

Theorem 1. *The control law (Eq. 9) makes the equilibrium point of the dynamical system introduced in Eq. (8) asymptotically stable.*

Proof. For this purpose, the positive definite function U_1 is assumed as

$$U_1 = \frac{1}{2}\left\{k_1 z_1^2 + k_2 z_2^2 + k_3 z_3^2\right\} \tag{11}$$

The derivative of this function can be obtained using Eq. (8) as

$$\begin{aligned} \dot{U}_1 = k_1 z_1 \dot{z}_1 + k_2 z_2 \dot{z}_2 + k_3 z_3 \dot{z}_3 = k_1 z_1 \left\{r_d z_2 + \Omega_1 - \Omega_2 z_3\right\} \\ + k_2 z_2 \left\{-r_d z_1 + (u_d + \Omega_1)\, z_3 + \Omega_2\right\} + k_3 z_3 \Omega_3 \end{aligned} \tag{12}$$

Simplifications yield

$$\dot{U}_1 = \Omega_1 \left(k_1 z_1 + k_2 z_2 z_3\right) + k_2 z_2 z_3 u_d + \Omega_2 \left(k_2 z_2 - k_1 z_1 z_3\right) + k_3 \Omega_3 z_3 + k_1 z_1 z_2 r_d - k_2 z_1 z_2 r_d \tag{13}$$

Expression $-k_3 \left|u_d\right| z_3$ is a stabilizer term and is used to stabilize z_3. Other terms have been used in order to convert the derivative of the Lyapunov function candidate (LFC) into at least a negative semidefined function. With these choices, the system inputs will be as Eq. (9) and the derivative of the LFC U_1 can be obtained as

$$\dot{U}_1 = -\left|u_d\right| \left\{k_1 z_1 + k_2 z_2 z_3\right\}^2 - \left|u_d\right| \left\{k_2 z_2 - k_1 z_1 z_3\right\}^2 - k_3 \left|u_d\right| z_3^2 \tag{14}$$

As can be seen, by choosing the positive control gains, the derivative of the LFC U_1 is a negative semidefined function. Therefore, U_1 is not an increasing function, and $z_i \left(i\colon 1 \rightarrow 3\right)$ are globally bounded. The derivative of the LFC became a negative semidefined function; therefore, the asymptotic stability of the system cannot be concluded. As mentioned in Property 1, u_d is continuous and its derivatives are uniformly bounded. In order to achieve the asymptotic stability, we use Barbalat Lemma.[42] In fact, it must be proved that the second derivative of the LFC is bounded. Therefore, the second derivative of the LFC U_1 is as

$$\begin{aligned} \ddot{U}_1 = -\dot{u}_d \frac{u_d}{\left|u_d\right|} \{k_1 z_1 + k_2 z_2 z_3\}^2 - 2\left|u_d\right| \left(k_1 z_1 + k_2 z_2 z_3\right) \{k_1 \left(r_d z_2 + \Omega_1 - z_3 \Omega_2\right) \\ + k_2 \left(-r_d z_1 + (u_d + \Omega_1)\, z_3 + \Omega_2\right) z_3 + k_2 z_2 \Omega_2\} - \dot{u}_d \frac{u_d}{\left|u_d\right|} \{k_2 z_2 - k_1 z_1 z_3\}^2 \\ - 2\left|u_d\right| \left(k_2 z_2 + k_1 z_1 z_3\right) \{k_2 \left(-r_d z_1 + (u_d + \Omega_1)\, z_3 + \Omega_2\right) \\ - k_1 \left(r_d z_2 + \Omega_1 - \Omega_2 z_3\right) z_3 - k_1 z_1 \Omega_3\} - \dot{u}_d \frac{u_d}{\left|u_d\right|} z_3^2 - 2\left|u_d\right| z_3 \Omega_2 \end{aligned} \tag{15}$$

Since $z_i (i\colon 1 \rightarrow 3)$ are globally bounded and according to Property 1, the reference kinematic inputs u_d, v_d, and r_d and their derivatives are continuous and globally bounded; therefore, it can be concluded that $\ddot{U}_1$ is bounded and according to the Barbalat Lemma, when t approaches infinity, U_1 approaches zero and as a result, the system is asymptotically stable.[43] Substituting control inputs from Eq. (9) into Eq. (10), system kinematic inputs $\mathcal{V} = \left[u\ v\ r\right]^T$ will be obtained. These kinematic control inputs are assumed as control commands for the design of the dynamic controller, and hence are displayed as $\mathcal{V}_c = \left[u_c\ v_c\ r_c\right]^T$ in the following.

4.3. Dynamic control

In dynamic control, the purpose is to obtain actuator torques to stabilize the dynamic control errors defined as $\varepsilon = \mathcal{V} - \mathcal{V}_c$ around the origin. Therefore, system dynamic input vector $F = \left[F_u\ F_v\ \tau_r\right]^T$ is proposed as

https://doi.org/10.1017/S0263574719001279 Published online by Cambridge University Press

$$F = H^{-1}\left\{\dot{\mathcal{V}}_c - \gamma + K\left(\mathcal{V}_c - \mathcal{V}\right)\right\} \tag{16}$$

where $\gamma = A\left[u \;\; v \;\; r\right]^T + B\left[vr \;\; ur \;\; uv\right]^T + D\left[u\,|u| \;\; v\,|v| \;\; r\,|r|\right]^T$ and $\mathrm{K} = \mathrm{diag}\left[k_1 \;\; k_2 \;\; k_3\right]$ is the controller gain matrix. Substituting Eq. (16) into Eq. (2) and simplifying, it can be concluded that

$$\dot{\mathcal{V}} - \dot{\mathcal{V}}_c + K\left(\mathcal{V} - \mathcal{V}_c\right) = 0 \tag{17}$$

Therefore, the system closed loop equation can be obtained as $\dot{\varepsilon} + K\varepsilon = 0$, which is a stable equation from the Routh–Hurwitz stability criterion, assuming a positive controller. Accordingly, the dynamic control inputs investigated based on Eq. (16) meet the requirements.

5. Formation Control

In this section, we introduce a control algorithm for the formation control of AUVs. The geometric model that is presented in this study assumes that robots use laser scanning sensors to find relative position of each other. In this way, each robot can find the distance and the angle of the line which connects itself to the leader of the group at any moment. For greater flexibility of the proposed model, the angle–distance geometry is used. In this sense, to determine the desirable position of each of the robots in the group, it is sufficient to determine the distance between the robot and the leader and the angle of the line between them with the horizon. Using this geometry, all types of formation systems can be described. It is assumed that the point P as a reference point of the robot is used for the formation control of the system. The i-th follower robot according to Fig. 2 with configuration variables $\xi_i = \left[x_i \;\; y_i \;\; \varphi_i\right]^T$ is aimed to follow the leader robot with configuration variables $\xi = \left[x \;\; y \;\; \varphi\right]^T$ and get the desired formation with the configuration variables $\xi_i^d = \left[x_i^d \;\; y_i^d \;\; \varphi_i^d\right]^T$. Therefore, the control inputs for navigating a follower robot must be determined in such a way that the relative distance and angle between the follower and the leader (which are shown in Fig. 2, respectively, with ρ_i and ϕ_i parameters) converge to their corresponding desirable values, that is, ρ_i^d and ϕ_i^d. The generalized coordinates of the i-th follower robot according to Fig. 2 are given as

$$\xi_i = \begin{bmatrix} x + \rho_i \cos\left(\phi_i + \varphi\right) \;\; - a\cos\varphi_i \\ y + \rho_i \sin\left(\phi_i + \varphi\right) \;\; - a\sin\varphi_i \\ \varphi_i \end{bmatrix} \tag{18}$$

Also, the desirable generalized coordinates of the i-th follower robot are obtained as

$$\xi_i^d = \begin{bmatrix} x + \rho_i^d \cos\left(\phi_i^d + \varphi\right) \;\; - a\cos\varphi_i \\ y + \rho_i^d \sin\left(\phi_i^d + \varphi\right) \;\; - a\sin\varphi_i \\ \varphi \end{bmatrix} \tag{19}$$

The relative distance between the leader and follower AUVs in terms of its components can be expressed as $\rho_i = \sqrt{\rho_{ix}^2 + \rho_{iy}^2}$. These components shown in Fig. 2 can be expressed according to the variables of the system as

$$\begin{aligned} \rho_{ix} &= x - x_i - a\cos\varphi_i = -\rho_i \cos\left(\phi_i + \varphi\right) \\ \rho_{iy} &= y - y_i - a\,sin\varphi_i = -\rho_i \sin\left(\phi_i + \varphi\right) \end{aligned} \tag{20}$$

where a is the distance between C_i and P_i shown in Fig. 2.

For the relative angle according to Fig. 2, it can be concluded

$$\phi_i = \tan^{-1}\frac{\rho_{iy}}{\rho_{ix}} \;\; - \varphi + \pi \tag{21}$$

Differentiation from ρ_i and ϕ_i and some simplifications yield the system formation dynamics as

$$\begin{aligned} \frac{\mathrm{d}\rho_i}{\mathrm{dt}} &= -u\cos\phi_i \;\; - v\sin\phi_i \;\; + u_i\cos\alpha_i \;\; + v_i\sin\alpha_i + \mathrm{ar}_i\sin\alpha_i \\ \frac{\mathrm{d}\phi_i}{\mathrm{dt}} &= \frac{1}{\rho_i}\left(u\sin\phi_i \;\; - v\cos\phi_i \;\; - u_i\sin\alpha_i \;\; - v_i\cos\alpha_i + \mathrm{ar}_i\cos\alpha_i\right) - r \end{aligned} \tag{22}$$

where $\alpha_i = \phi_i + \varphi - \varphi_i$.

https://doi.org/10.1017/S0263574719001279 Published online by Cambridge University Press

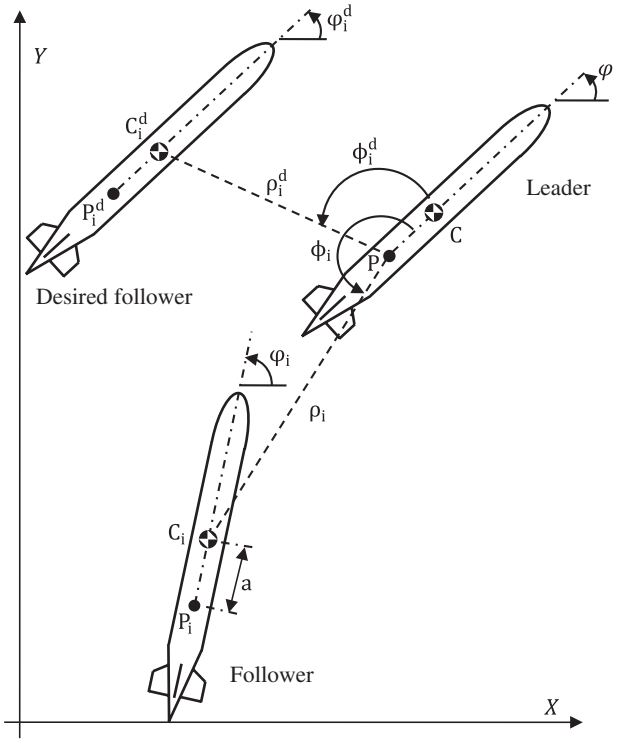

Fig. 2. Formation control for a group of AUVs

The system formation error vector is defined as

$$e_i = \mathcal{T}(\varphi_i)\left\{\xi_i^d - \xi_i\right\} \tag{23}$$

Using Eq. ı(20), the formation error signal of the i-th follower $e_i = \left[\, e_{ix} \;\; e_{iy} \;\; e_{i\varphi} \,\right]^T$ can be rewritten as

$$e_i = \begin{bmatrix} \rho_i^d \cos\left(\phi_i^d + \varphi - \varphi_i\right) & -\rho_i^d \cos\alpha_i \\ \rho_i^d \sin\left(\phi_i^d + \varphi - \varphi_i\right) & -\rho_i^d \sin\alpha_i \\ \varphi_i^d - \varphi_i & \end{bmatrix} \tag{24}$$

The formation error dynamics of the system is obtained by the time derivative of Eq. (24) which is obtained as

$$\frac{\mathrm{d}e_i}{\mathrm{dt}} = \mathcal{T}(\varphi_i)(\xi_i^d - \xi_i) + \mathcal{T}(\varphi_i)(\dot{\xi}_i^d - \dot{\xi}_i) \tag{25}$$

Simplifying the above equation and assuming $\mathrm{d}\rho_i^d/\mathrm{dt} = \mathrm{d}\phi_i^d/\mathrm{dt} = 0$ yields

$$\begin{aligned} \frac{\mathrm{d}e_i}{\mathrm{dt}} = &\begin{bmatrix} \cos\left(\varphi - \varphi_i\right) & -\sin\left(\varphi - \varphi_i\right) & -\rho_i^d \sin\left(\phi_i^d + \varphi - \varphi_i\right) \\ \sin\left(\varphi - \varphi_i\right) & \cos(\varphi - \varphi_i) & \rho_i^d \cos\left(\phi_i^d + \varphi - \varphi_i\right) \\ 0 & 0 & 0 \end{bmatrix} \begin{bmatrix} u \\ v \\ r \end{bmatrix} \\ &+ \begin{bmatrix} -1 & -\sin 2\alpha_i & e_{iy} \\ 0 & \cos 2\alpha_i & -(a + e_{ix}) \\ 0 & 0 & -1 \end{bmatrix} \begin{bmatrix} u_i \\ v_i \\ r_i \end{bmatrix} + \begin{bmatrix} 0 \\ 0 \\ r_i^d \end{bmatrix} \end{aligned} \tag{26}$$

In the above equations, the inputs for formation control $\mathcal{V}_i = \left[\, u_i \;\; v_i \;\; r_i \,\right]^T$ should be investigated in order to stabilize the system formation error dynamics around the origin. To this end, using feedback linearization, nonlinear terms are eliminated and the control inputs are chosen as

$$\mathcal{V}_i = \begin{bmatrix} \cos\left(\varphi - \varphi_i\right) & -\sin\left(\varphi - \varphi_i\right) & -\rho_i^d \sin\left(\phi_i^d + \varphi - \varphi_i\right) \\ 0 & 0 & 0 \\ \frac{1}{a}\sin\left(\varphi - \varphi_i\right) & \frac{1}{a}\cos\left(\varphi - \varphi_i\right) & \frac{\rho_i^d}{a}\cos\left(\phi_i^d + \varphi - \varphi_i\right) \end{bmatrix} \mathcal{V} + \begin{bmatrix} \gamma_1 & 0 & 0 \\ 0 & 0 & 0 \\ 0 & \frac{\gamma_2}{a} & \frac{\gamma_3}{a} \end{bmatrix} e_i \tag{27}$$

https://doi.org/10.1017/S0263574719001279 Published online by Cambridge University Press

Table I. Parameters of the underwater robot.

Parameter	Symbol	Value	Unit
AUV mass	m	185	kg
Rotational inertia	I_z	50	$\text{kg} \cdot \text{m}^2$
Surge linear drag	X_u	70	$\text{kg} \cdot \text{s}^{-1}$
Surge quadratic drag	$X_{u\|u\|}$	100	$\text{kg} \cdot \text{m}^{-1}$
Sway linear drag	Y_v	100	$\text{kg} \cdot \text{s}^{-1}$
Sway quadratic drag	$Y_{v\|v\|}$	200	$\text{kg} \cdot \text{m}^{-1}$
Yaw linear drag	N_r	50	$\text{kg} \cdot \text{m}^2 \cdot \text{s}^{-1}$
Yaw quadratic drag	$N_{r\|r\|}$	100	$\text{kg} \cdot \text{m}^2$
Added mass	$X_{\dot{u}}$	−30	kg
Added mass	$Y_{\dot{v}}$	−80	kg
Added mass	$N_{\dot{r}}$	−30	$\text{kg} \cdot \text{m}^2$

where $\gamma_i (i: 1 \rightarrow 3)$ are system controller gains. Substituting these control inputs in Eq. (26), based on feedback linearization method r_i^d is obtained as

$$r_i^d = \frac{1}{a}\left\{u \sin(\varphi - \varphi_i) + v\cos(\varphi - \varphi_i) + \rho_i^d r \cos\left(\phi_i^d + \varphi - \varphi_i\right) + 2\gamma_2 e_{iy}\right\} \tag{28}$$

Therefore, system error dynamics can be calculated as

$$\frac{\mathrm{d}e_i}{\mathrm{dt}} = \begin{bmatrix} \gamma_1 & r_i & 0 \\ r_i & -\gamma_2 & -\gamma_3 \\ 0 & \frac{-\gamma_2}{a} & \frac{-\gamma_3}{a} \end{bmatrix} e_i \tag{29}$$

Now, the LFC is chosen as $U_2 = \frac{1}{2}\left(e_{ix}^2 + e_{iy}^2\right) + \frac{a\gamma_3 e_{i\varphi}^2}{2\gamma_2}$ which is a positive definite function and can also be expressed as

$$U_2 = \frac{1}{2} e_i^T \operatorname{diag}\left(\begin{bmatrix} 1 & 1 & \frac{a\gamma_3}{\gamma_2} \end{bmatrix}\right) e_i \tag{30}$$

The time derivative of the LFC can be obtained as

$$\begin{aligned} \dot{U}_2 &= e_{ix}\dot{e}_{ix} + e_{iy}\dot{e}_{iy} + \frac{a\gamma_3}{\gamma_2} e_{i\varphi}\dot{e}_{i\varphi} = r_i e_{ix} e_{iy} - \gamma_1 e_{ix}^2 - r_i e_{ix} e_{iy} - \gamma_2 e_{iy}^2 - \gamma_3 e_{iy} e_{i\varphi} \\ &+ \frac{a\gamma_3}{\gamma_2}\left(\frac{\gamma_2}{a} e_{iy} e_{i\varphi} - \frac{\gamma_3}{a} e_{i\varphi}^2\right) = -\gamma_1 e_{ix}^2 - \gamma_2 e_{iy}^2 - \frac{\gamma_3^2}{\gamma_2} e_{i\varphi}^2 < 0 \end{aligned} \tag{31}$$

Therefore, the derivative of the LFC is negative definite. Therefore, using the proposed algorithm, the formation control errors will be stabilized gradually and follower AUVs follow their desired formations relative to the leader.

6. Obtained Results

In this section, the achieved results of the proposed control algorithm are reported in order to evaluate the efficiency of the proposed algorithm on formation control of underwater leader and follower AUVs. It is aimed that the leader AUV follows the desired reference path and at the same time the followers stand in a given configuration relative to it. The values of the AUV hydrodynamic parameters and the added masses are presented in Table I.[10]

The control parameters are presented in Table II. It should be noted that the controller gains are positive constants that can magnify the error variables and their influence in the control algorithm satisfying the closed loop stability. Larger control gains lead to better responses, that is, lower settling times and faster convergence of the responses, but causes higher control inputs. On the other hand, fewer gains lead to the poor responses, that is, fluctuating responses, higher settling times, higher overshoots in system responses, but lower control inputs. Accordingly, there exist a compromise between these effects and the controller gains for having both the appropriate performance and reasonable control inputs which are selected using the trial and error method, while the closed loop

https://doi.org/10.1017/S0263574719001279 Published online by Cambridge University Press

Table II. Control parameters.

Parameter	Symbol	Value	Unit
PC distance	a	0.5	m
Kinematic control gains	$k_i(i: 1\rightarrow 3)$	10, 10, 60	–
Dynamic control gains	$k_i(i: 1\rightarrow 3)$	10, 10, 10	–
Formation control gains	$\beta_i(i: 1\rightarrow 3)$	50, 70, 20	–
Parameters of formation control 1	$\rho_i^d(i: 1\rightarrow 2)$	2, 2	m
Parameters of formation control 1	$\phi_i^d(i: 1\rightarrow 2)$	$\pi/2, -\pi/2$	rad
Parameters of formation control 2	ρ_i^d $(i: 1\rightarrow 5)$	3, 2, 3, 2, 2	m
Parameters of formation control 2	ϕ_i^d $(i: 1\rightarrow 5)$	$\pi/2, 3\pi/4, -\pi/2, -3\pi/4, \pi$	rad
Parameters of formation control 3	$\rho_i^d(i: 1\rightarrow 2)$	4, 4	rad
Parameters of formation control 3	$\phi_i^d = \overline{\phi}_i^d - \theta_r$ $(i: 1\rightarrow 2)$	$\overline{\phi}_i^d = 0, \pi$ or $\pi/2, 3\pi/2$	rad
Parameters of formation control 4	ρ_i^d $(i: 1\rightarrow 5)$	3, 3, 3, 3, 3	m
Parameters of formation control 4	ϕ_i^d $(i: 1\rightarrow 5)$	$2\pi/5, 4\pi/5, 6\pi/5, 8\pi/5, 2\pi$	rad
Parameters of formation control 5	ρ_i^d $(i: 1\rightarrow 5)$	3, 3, 3, 3, 3	m
Parameters of formation control 5	ϕ_i^d $(i: 1\rightarrow 5)$	$5\pi/3, 11\pi/6, 13\pi/6, 7\pi/3, 2\pi$	rad

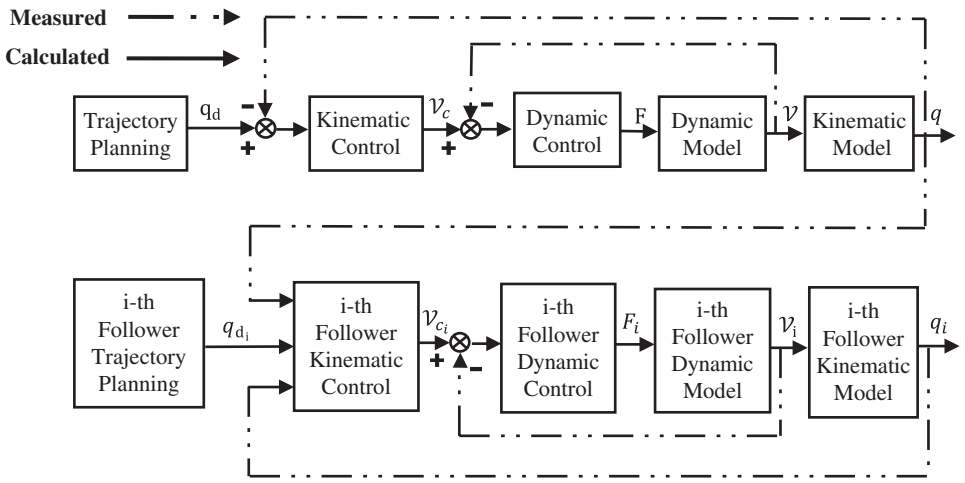

Fig. 3. Block diagram for the formation control of AUVs

system performance and the amount of control inputs are checked simultaneously. On the other hand, larger control gains will cause higher control inputs and vice versa. Therefore, the control gains for having both appropriate performance and reasonable control inputs are selected using the trial and error and simultaneously analyzing the closed loop system performance and the amount of control inputs. The control block diagram is presented in Fig. 3.

Since the stability of the tracking control (Eqs. (14), (15), and (17)) and robot formation control (Eq. (31)) was proved, and consequently, it is expected that the robot tracking errors and the robot formation control errors beginning from different initial configurations converge to zero after a limited time and transient responses of system be eliminated and the desired formation be followed in tracking reference trajectories. The reference trajectory equation is assumed as $y_d = 2\{5+\cos(a\frac{t}{50})\}\sin(6\frac{t}{50}+b)$, $x_d = 2\{5+\cos(a\frac{t}{50})\}\cos(6\frac{t}{50}+b)$ where $a = 18$ and $b = -\frac{\pi}{6}$ generate three-corner trajectory presented in Fig. 4 and $a = 24$ and $b = 0$ create a four-corner trajectory depicted in Fig. 10.

Formation 1. In this formation, a leader and two followers make a triangular formation in tracking three-corner trajectories. The parameters of this formation can be seen in Table II. The trajectory of the leader and follower AUVs in tracking the reference path is depicted in Fig. 4. The tracking control

https://doi.org/10.1017/S0263574719001279 Published online by Cambridge University Press

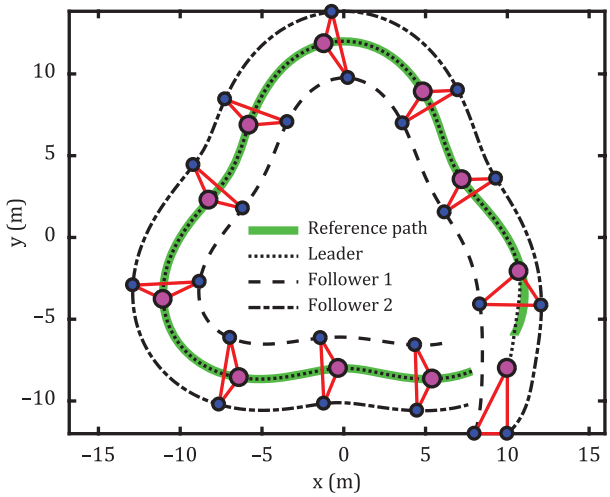

Fig. 4. Triangular formation control of AUVs in tracking the three-corner reference path (formation 1).

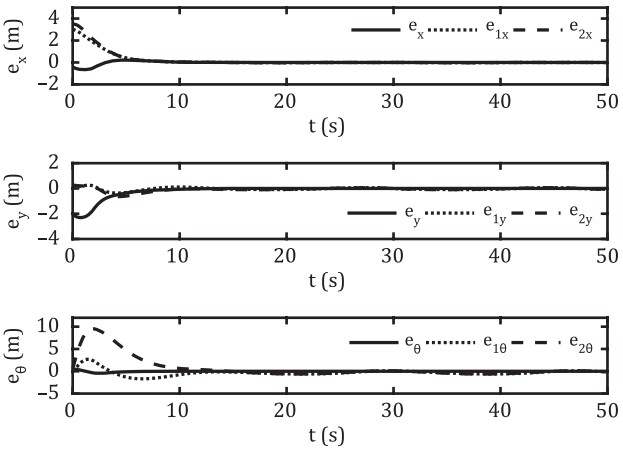

Fig. 5. Error signals for formation control of AUVs in tracking three-corner reference path.

error of the leader robot and the formation control errors for the followers are presented in Fig. 5. In Fig. 6, kinematic control inputs (including u, v, and r) and, in Fig. 7, dynamic control inputs (including F_u, F_v, and τ_r) are shown. Leader AUV (in magenta) followed reference path (in green), and follower AUVs (in blue) followed leader in the defined desired formation. The red lines represent the formation of AUVs. The desired distance and angle between leader and followers are shown in Table II.

In Fig. 4, it is observed that the reference path is tracked by the leader robot beginning from an initial condition. Similarly, two follower AUVs after their transient responses reach and follow their desired formations.

Comparing Figs. 4 and 5, it is also clear that the follower 1 with an initial error of about 3 m, follower 2 with an initial error of about 4 m, and the leader AUV with an initial error of about 2 m began to move and at about 11 s, control errors have almost been eliminated, and the AUVs have made their perfect formation in following the reference path in the Cartesian space.

The control inputs are smooth and have reasonable values and amplitudes and rate of variation, and at time $t = 0$, the inputs do not overshoot. This indicates the appropriate choice of control gains that caused to have proper control inputs with proper closed loop system functionality.

Formation 2. In this formation, a leader and four followers make a pentagon formation in tracking three- and four-corner trajectories. The parameters are specified in Table II. In Figs. 8–10 as it can be seen, AUVs beginning from different initial configurations converge the desired defined formation

https://doi.org/10.1017/S0263574719001279 Published online by Cambridge University Press

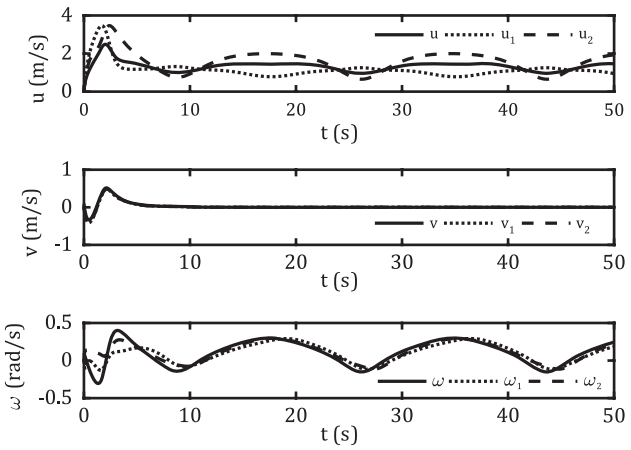

Fig. 6. Kinematic control inputs of the leader and follower AUVs.

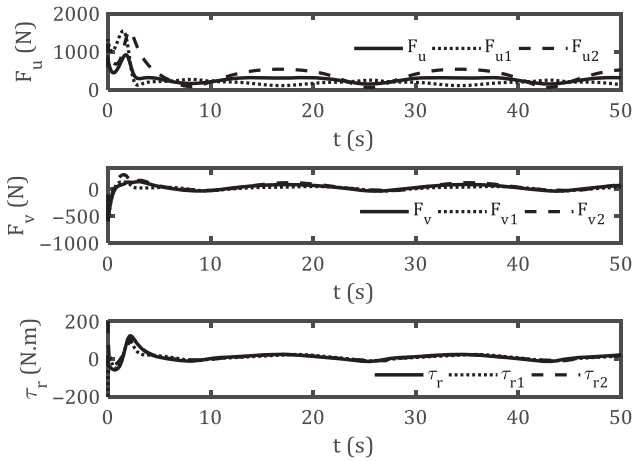

Fig. 7. Dynamic control inputs of the leader and follower AUVs.

either they are near to the reference path or far from it. The red lines show the desired formation which is achieved along the trajectory using the proposed control method.

In Fig. 8, all AUVs started from $y = -18$ and different x coordinates and they tracked the desired configurations gradually. Similarly, in Fig. 9, the performance of the controller is represented for the AUVs beginning from initial configurations far from the reference path. Finally, in Fig. 10, the initial configurations are chosen far from each other and still the control algorithm operates effectively. Consequently, neglecting the initial configurations, all the AUVs follow the desired formation in a limited time.

Formation 3. In this formation, a leader and two followers make a time-varying triangular formation in tracking four-corner trajectories. The parameters of this formation are given in Table II. In Figs. 11 and 12, the trajectory of the AUVs is represented for the time-varying formations in tracking four-corner reference trajectories. In Figs. 11 and 12, the desired angles between leader and followers are $-\theta_r$, $\pi - \theta_r$ and $\frac{\pi}{2} - \theta_r$, $\frac{3\pi}{2} - \theta_r$, respectively.

It is also clear from the comparison of two formations that the reference path in the Cartesian space has been extended for follower AUVs in horizontal and vertical directions, and the proposed algorithm operates efficiently.

Formation 4. In this formation, as can be seen in Fig. 13, a leader and five followers make a pentagon formation in tracking the four-corner trajectories. The parameters are specified in Table II. In this formation, the leader robot stays in the heart of the formation and followers surround the leader.

https://doi.org/10.1017/S0263574719001279 Published online by Cambridge University Press

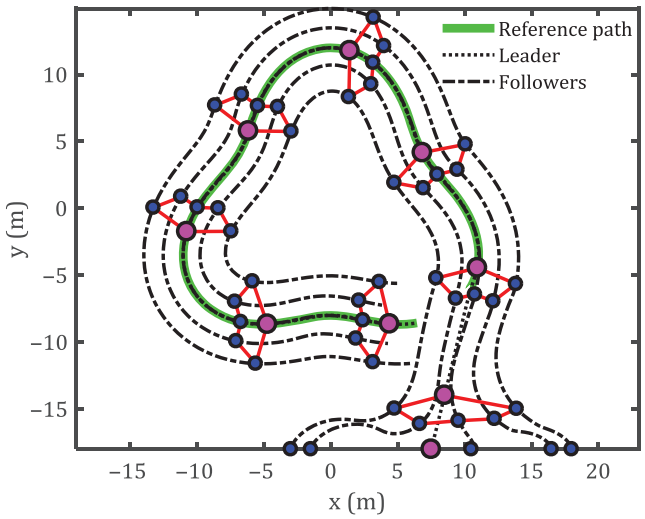

Fig. 8. Pentagon formation control of AUVs in tracking the three-corner path (formation 2-1).

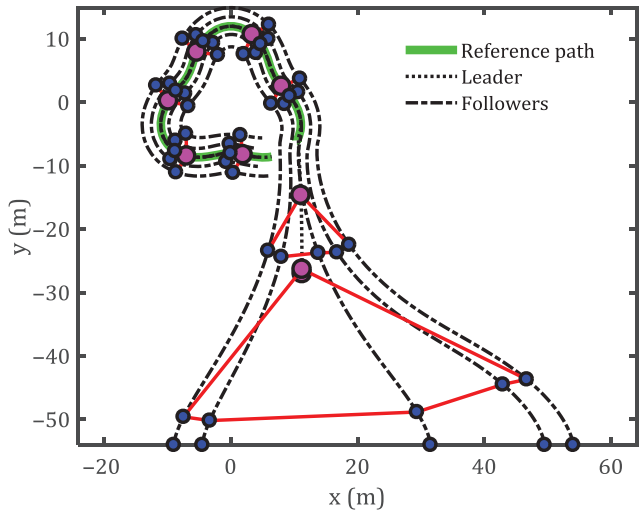

Fig. 9. Pentagon formation control of AUVs in tracking the three-corner path, with initial configurations far from the desired trajectory (formation 2-2).

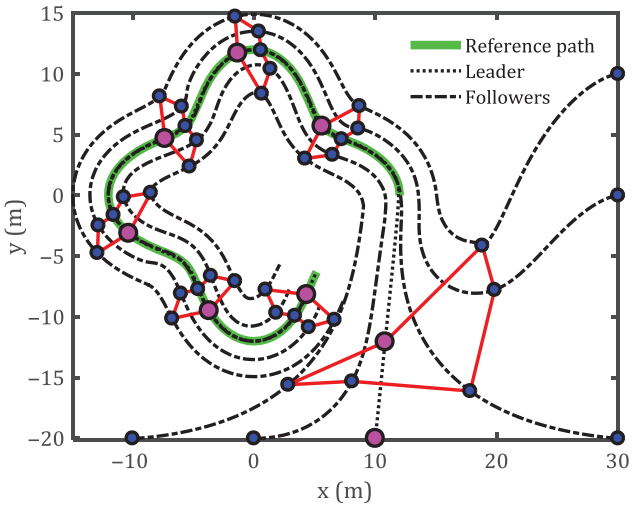

Fig. 10. Pentagon formation control of AUVs in tracking the four-corner path with scattered initial configurations (formation 2-3).

https://doi.org/10.1017/S0263574719001279 Published online by Cambridge University Press

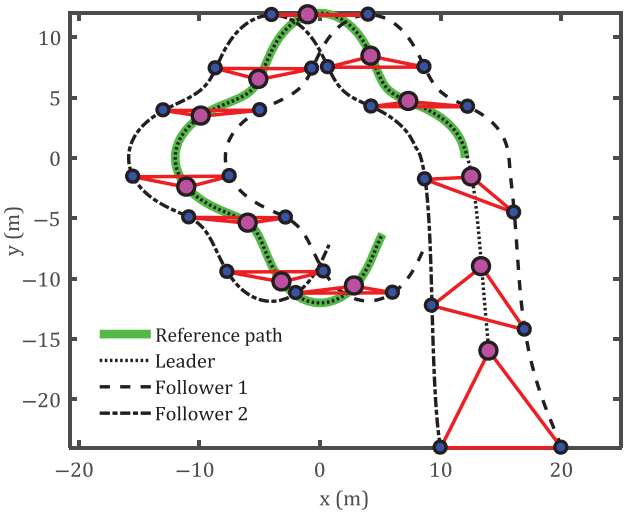

Fig. 11. Time-varying triangular formation control of AUVs in tracking the four-corner path (formation 3-1).

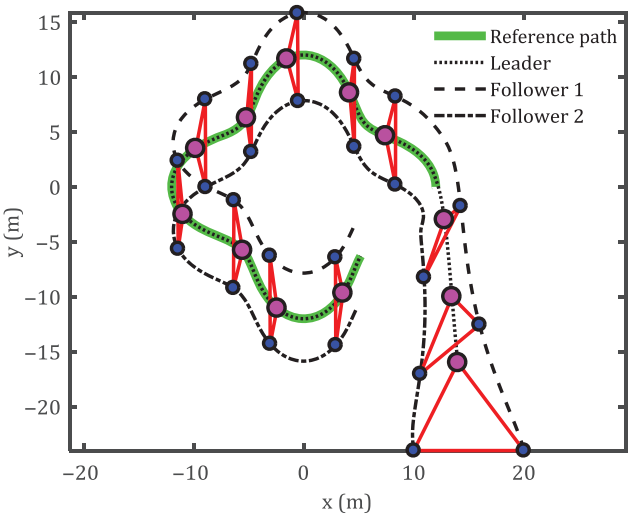

Fig. 12. Time-varying triangular formation control of AUVs in tracking the four-corner path (formation 3-2).

Formation 5. In this formation, as can be seen in Fig. 14, a leader and five followers make a crescent formation in tracking the three-corner trajectories. The parameters are given in Table II. In this formation, followers move ahead of the leader but the leader navigates them in order to get the right configuration.

Robustness to Uncertainties and Disturbances: As another study, the AUV is affected by external disturbances as $F_d = 2500\,[1\ 1\ 1]^T\{H(t-20) - H(t-25)\}$ which is applied parallel to the dynamic input F, where $H(t)$ is the unit step function. Also, the mass parameters are assumed to be changed as $\eta \rightarrow \{1 + 15\,H(t-15) - 15\,H(t-30)\}\,\eta$, where η represents system parameters as $\eta \in \{m_{11},\ m_{22}\ m_{33}\}$. In Fig. 15, the AUV motion in tracking three corners desired trajectory in the presence of external disturbances is demonstrated. In Fig. 16, the AUV motion in tracking three corners desired trajectory in the presence of parametric uncertainties is shown.

These uncertainties are rarely expected in real systems. As can be seen, the proposed control algorithm can compensate the effects of external disturbances and parametric uncertainties.

Tracking the Circular and the Circular Modulated with a Sinusoidal Wave Trajectories: In this study, formation control in tracking the circular (Fig. 17) and the circular modulated with a sinusoidal wave trajectory (Fig. 18) are analyzed.

https://doi.org/10.1017/S0263574719001279 Published online by Cambridge University Press

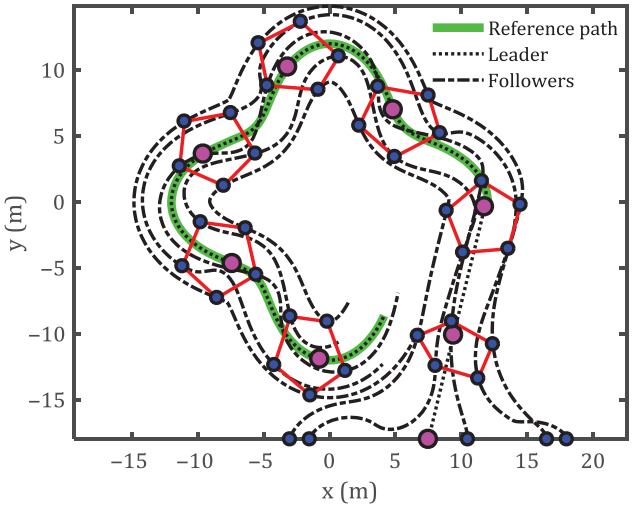

Fig. 13. Pentagon formation control of AUVs in tracking the four-corner path (formation 4).

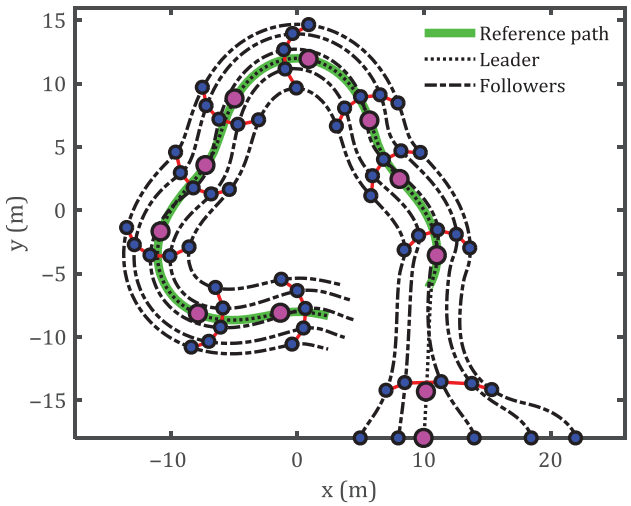

Fig. 14. Crescent formation control of AUVs in tracking the three-corner path (formation 5).

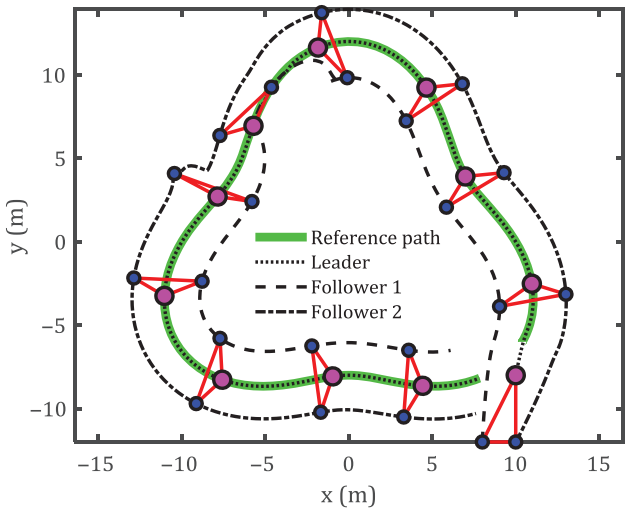

Fig. 15. Triangular formation control of AUVs in tracking the three-corner reference path in the presence of external disturbances.

https://doi.org/10.1017/S0263574719001279 Published online by Cambridge University Press

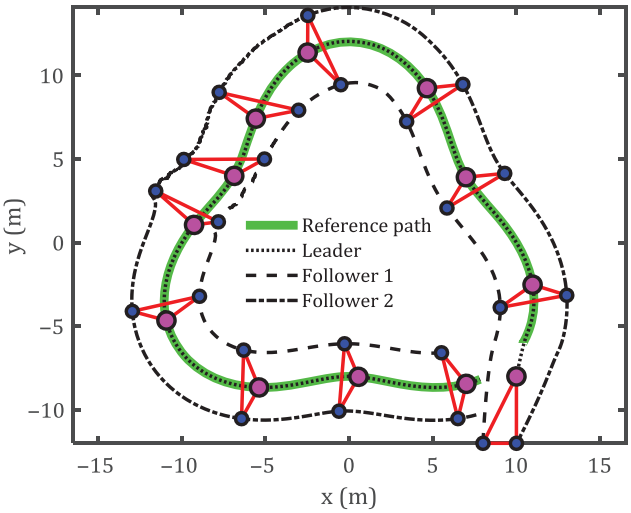

Fig. 16. Triangular formation control of AUVs in tracking the three-corner reference path in the presence of parametric uncertainties.

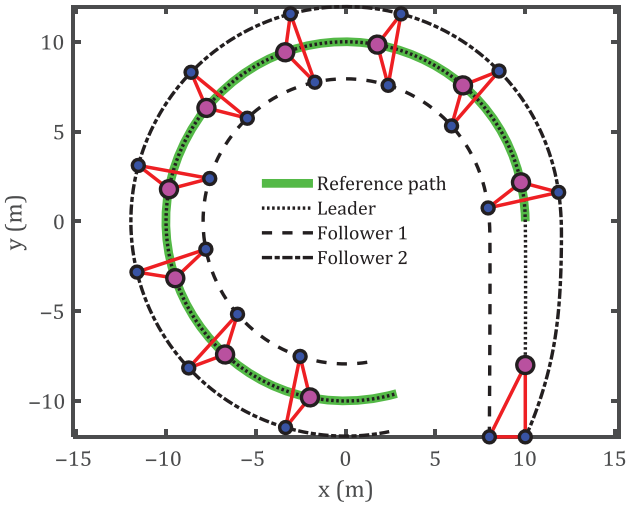

Fig. 17. Triangular formation control of AUVs in tracking the circular reference path.

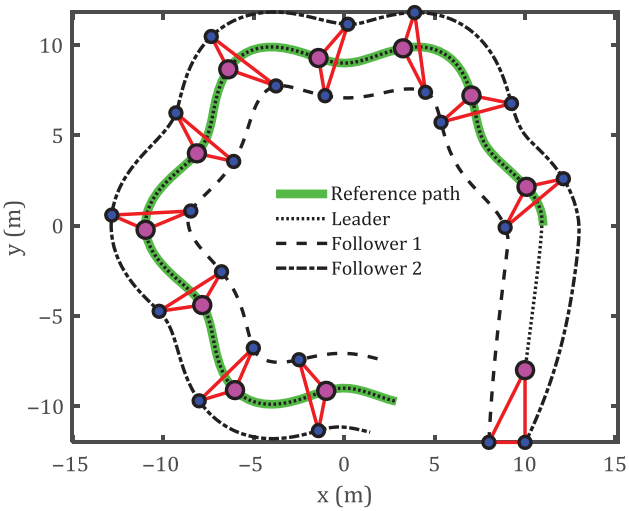

Fig. 18. Triangular formation control of AUVs in tracking the circular path modulated with a sinusoidal wave.

https://doi.org/10.1017/S0263574719001279 Published online by Cambridge University Press

The results show that the formation control in tracking reference trajectories is effectively achieved utilizing the proposed algorithm for a group of underwater robots. As can be seen, the leader robot, beginning from the initial configuration, efficiently follows various reference paths in a limited time and is placed on an appropriate margin relatively. The control errors are converged to zero gradually as was expected with the stability proof at different stages of the control algorithm. As a result, the follower AUVs in their specified formations are placed in the desired configuration relative to the leader robot. Generated control inputs have appropriate values and are within reasonable limits as applied torques.

7. Conclusion

In this paper, a new Lyapunov-based method for dynamic formation control of the AUVs in tracking reference trajectories as a nonlinear dynamical system is proposed. First, system mathematical equations were obtained. Then, appropriate reference trajectories were produced for the leader AUV, and a feedback kinematic controller is proposed for the leader robot. Next, a dynamic control law was developed to generate actuator torques of the leader. Afterward, a formation control procedure was investigated for the group of AUVs. Consequently, the follower AUVs stay in a desired configuration associated with the leader AUV in tracking reference trajectories. The stability of the proposed method was investigated utilizing the Lyapunov theory for kinematic, dynamic, and formation controllers. The presented method capabilities were analyzed in tracking different formations applying parametric uncertainties and external disturbances. The results confirm the efficiency of the proposed formation control algorithm for the AUVs in tracking reference trajectories.

References

1. F. Tajdari, E. Khodabakhshi, M. Kabganian and A. Golgouneh, "Switching Controller Design to Swing-up a Two-Link Underactuated Robot," *2017 IEEE 4th International Conference on Knowledge-Based Engineering and Innovation (KBEI)*, Tehran, Iran (2017) pp. 0595–0599.
2. F. Tajdari, M. Kabganian, E. Khodabakhshi and A. Golgouneh, "Design, Implementation and Control of a Two-Link Fully-Actuated Robot Capable of Online Identification of Unknown Dynamical Parameters Using Adaptive Sliding Mode Controller," *2017 Artificial Intelligence and Robotics (IRANOPEN)*, Qazvin, Iran (2017) pp. 91–96.
3. A. Keymasi Khalaji, "Modeling and control of uncertain multibody wheeled robots," *Multibody Syst. Dyn.* **46**(3), 257–279 (2019).
4. A. Keymasi Khalaji, "PID-based target tracking control of a tractor-trailer mobile robot," *Proc. Inst. Mech. Eng. Part C J. Mech. Eng. Sci.* **233**(13), 4776–4787 (2019).
5. A. Keymasi Khalaji and S. A. A. Moosavian, "Switching control of a Tractor-Trailer wheeled robot," *Int. J. Robot. Auto*. **30**(2), 1–9 (2015).
6. A. Karimi and R. Hasanzadeh Ghasemi, "Equipping of a hovering type autonomous underwater vehicle with ballast tanks and its effect on degrees of freedom," *Modares Mech. Eng.* **17**(7), 397–404 (2017).
7. H. Ashrafiuon, K. R. Muske, L. C. McNinch and R. A. Soltan, "Sliding-mode tracking control of surface vessels," *IEEE Trans. Ind. Electron.* **55**(11), 4004–4012 (2008).
8. L. Wang, L.-J. Zhang, H.-M. Jia and H.-B. Wang, "Horizontal Tracking Control for AUV Based on Nonlinear Sliding Mode," *2012 International Conference on Information and Automation (ICIA),* Shenyang, China (2012) pp. 460–463.
9. H. Joe, M. Kim and S.-C. Yu, "Second-order sliding-mode controller for autonomous underwater vehicle in the presence of unknown disturbances," *Nonlinear Dyn.* **78**(1), 183–196 (2014).
10. T. Elmokadem, M. Zribi and K. Youcef-Toumi, "Terminal sliding mode control for the trajectory tracking of underactuated Autonomous Underwater Vehicles," *Ocean Eng.* **129**, 613–625 (2017).
11. Y. Chen, R. Zhang, X. Zhao and J. Gao, "Adaptive fuzzy inverse trajectory tracking control of underactuated underwater vehicle with uncertainties," *Ocean Eng.* **121**, 123–133 (2016).
12. K. D. Do, J. Pan and Z. Jiang, "Robust and adaptive path following for underactuated autonomous underwater vehicles," *Ocean Eng.* **31**(16), 1967–1997 (2004).
13. J.-S. Wang and C. G. Lee, "Self-adaptive recurrent neuro-fuzzy control of an autonomous underwater vehicle," *IEEE Trans. Robot. Auto.* **19**(2), 283–295 (2003).
14. B. K. Sahu and B. Subudhi, "Adaptive tracking control of an autonomous underwater vehicle," *Int. J. Auto. Comput.* **11**(3), 299–307 (2014).
15. E. Sebastián and M. A. Sotelo, "Adaptive fuzzy sliding mode controller for the kinematic variables of an underwater vehicle," *J. Intell. Rob. Syst.* **49**(2), 189–215 (2007).
16. F. S. Tabataba'i-Nasab, A. Keymasi Khalaji and S. A. A. Moosavian, "Adaptive nonlinear control of an autonomous underwater vehicle," *Trans. Inst. Meas. Control.* **41**(11), 3121–3131 (2019).
17. J. Yuh, "A neural net controller for underwater robotic vehicles," *IEEE J. Oceanic Eng.* **15**(3), 161–166 (1990).

https://doi.org/10.1017/S0263574719001279 Published online by Cambridge University Press

18. X. Liang, L. Wan, J. I. Blake, R. A. Shenoi and N. Townsend, "Path following of an underactuated AUV based on fuzzy backstepping sliding mode control," *Int. J. Adv. Robot. Syst.* **13**(3), 122 (2016).
19. T. Balch and R. C. Arkin, "Behavior-based formation control for multirobot teams," *IEEE Trans. Robot. Auto.* **14**(6), 926–939 (1998).
20. K. Alipour and A. Abbaspour, "The effect of remote center compliance parameters on formation control of cooperative wheeled mobile robots for object manipulation," *Int. J. Control Auto. Syst.* **16**(1), 306–317 (2018).
21. J. Cullen, E. Shaw and H. A. Baldwin, "Methods for measuring the three-dimensional structure of fish schools," *Anim. Behav.* **13**(4), 534–543 (1965).
22. A. Abbaspour, S. A. A. Moosavian and K. Alipour, "Formation control and obstacle avoidance of cooperative wheeled mobile robots," *Int. J. Robot. Auto.* **30**(5), 418–428 (2015).
23. R. R. Murphy, "Human-robot interaction in rescue robotics," *IEEE Trans. Syst. Man. Cybern Part C Appl. Rev.* **34**(2), 138–153 (2004).
24. I. R. Nourbakhsh, K. Sycara, M. Koes, M. Yong, M. Lewis and S. Burion, "Human-robot teaming for search and rescue," *IEEE Pervasive Comput.* **4**(1), 72–78 (2005).
25. A. Y. Lam, Y.-W. Leung, and X. Chu, "Autonomous-vehicle public transportation system: Scheduling and admission control," *IEEE Trans. Intell. Trans. Syst.* **17**(5), 1210–1226 (2016).
26. K. Margellos and J. Lygeros, "Toward 4-D trajectory management in air traffic control: A study based on monte carlo simulation and reachability analysis," *IEEE Trans. Control Syst. Tech.* **21**(5), 1820–1833 (2013).
27. D. Voth, "A new generation of military robots," *IEEE Intelligent Systems.* **19**(4), 2–3 (2004).
28. I. Baturone, F. J. Moreno-Velo, S. Sanchez-Solano and A. Ollero, "Automatic design of fuzzy controllers for car-like autonomous robots," *Fuzzy Syst. IEEE Trans.* **12**(4), 447–465 (2004).
29. M. Egerstedt and X. Hu, "Formation constrained multi-agent control," *IEEE Trans. Rob. Autom.* **17**(6), 947–951 (2001).
30. H. Yamaguchi, "A distributed motion coordination strategy for multiple nonholonomic mobile robots in cooperative hunting operations," *Robot. Auto. Syst.* **43**(4), 257–282 (2003).
31. A. Bazoula, M. Djouadi and H. Maaref, "Formation control of multi-robots via fuzzy logic technique," *Int. J. Comput. Commun. Control.* **3**(3), 179–184 (2008).
32. A. Bazoula and H. Maaref, "Fuzzy separation bearing control for mobile robots formation," *Proc. World Acad. Sci.* **1**(5), 1–7 (2007).
33. X. Li, J. Xiao and Z. Cai, "Backstepping Based Multiple Mobile Robots Formation Control," *2005 IEEE/RSJ International Conference on Intelligent Robots and Systems (IROS 2005)*, Edmonton, Canada (2005) pp. 887–892.
34. J. Sanchez and R. Fierro, "Sliding Mode Control for Robot Formations," *2003 IEEE International Symposium on Intelligent Control*, Houston, TX, USA (2003) pp. 438–443.
35. Z. Hou and I. Fantoni, "Distributed Leader-Follower Formation Control for Multiple Quadrotors with Weighted Topology," *2015 10th System of Systems Engineering Conference(SoSE)*, San Antonio, TX, USA (2015) pp. 256–261.
36. A. Soni and H. Hu, "Formation control for a fleet of autonomous ground vehicles: A survey," *Robotics* **7**(4), 67 (2018).
37. L. Consolini, F. Morbidi, D. Prattichizzo and M. Tosques, "A Geometric Characterization of Leader-Follower Formation Control," *Proceedings 2007 IEEE International Conference on Robotics and Automation*, Roma, Italy (2007) pp. 2397–2402.
38. L. Consolini, F. Morbidi, D. Prattichizzo and M. Tosques, "Leader–follower formation control of nonholonomic mobile robots with input constraints," *Automatica* **44**(5), 1343–1349 (2008).
39. J. P. Desai, J. P. Ostrowski and V. Kumar, "Modeling and control of formations of nonholonomic mobile robots," *IEEE Trans. Robot. Auto.* **17**(6), 905–908 (2001).
40. Y.-H. Chang, C.-W. Chang, C.-L. Chen and C.-W. Tao, "Fuzzy sliding-mode formation control for multi-robot systems: Design and implementation," *IEEE Trans. Syst. Man Cybern. Part B (Cybern.)* **42**(2), 444–457 (2012).
41. F. Repoulias and E. Papadopoulos, "Planar trajectory planning and tracking control design for underactuated AUVs," *Ocean Eng.* **34**(11–12), 1650–1667 (2007).
42. J.-J. E. Slotine and W. Li, *Applied Nonlinear Control,* vol. 199 (Prentice Hall, Englewood Cliffs, NJ, 1991).
43. H. K. Khalil, *Nonlinear Systems* (Prentice Hall, Englewood Cliffs, NJ, 2002) pp. 167–191.